

Flood risk of a touristic island beach under Climate Change: Komi beach Chios

Chatzistratis D¹., Monioudi I.N.¹, Chalazas T.¹, Andreadis O.P.¹, Moschopoulos K.¹, Chatzipavlis A.E.^{1,2}, Psarros F.¹, Velegrakis A.F.¹

(1) Department of Marine Sciences, University of the Aegean, University Hill, 81100 Mytilene, Greece, mard20007@aegean.gr (2) Department of Physics and Earth Sciences, University of Ferrara, Via Saragat 1, 44122 Ferrara, Italy

Research Highlights

Assessment of beach flood risk using open source geospatial data and models.

Introduction

Coastal floods from extreme marine events have had increasing impacts on the coastal natural and human ecosystems, causing coastline changes, biodiversity losses, human mortality, increased health risks and poverty and induced coastal infrastructure/asset damages (IPCC, 2023). Under climate change, the frequency of extreme events is projected to increase and expose annually a large part of the global coastline to the current 1 in 100 years Extreme Sea Level by 2100 (Vousdoukas *et al.*, 2018). ‘Sandy’ shorelines (i.e., the low-lying coasts built on sediments—beaches), which comprise a large segment of the global coastline (Luijendijk *et al.*, 2021) will be particularly vulnerable. In addition to their own importance as ecosystems, beaches form natural buffers that protect backshore ecosystems, infrastructure, and assets from coastal flooding (Toimil *et al.*, 2023); they also have high hedonic/recreational value, contributing very significantly to the tourism sector due to the current dominance of the ‘Sun, Sea, and Sand—3S’ model (UNWTO, 2024). Beaches in touristic islands face increased vulnerability to coastal flooding, due to their generally limited width, scarce sediment supply and the high potential exposure to coastal flooding of their backshore infrastructure and services (Brett, 2021). However, the flood assessment of beaches, presents certain challenges due to the need for accurate geospatial information, as well as the accuracy/costs of the used models (Almar *et al.*, 2021).

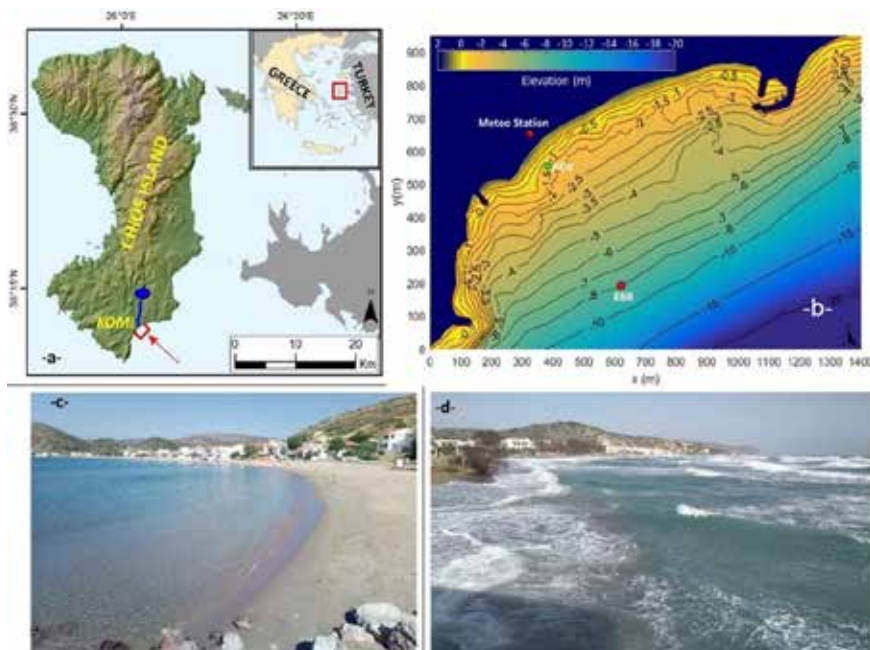


Figure 1. (a) Chios island and Komi beach, showing Katraris river and dam (blue line and circle). (b) Beach nearshore topography/bathymetry. Photos of Komi beach, (c) from the ENE under calm conditions and (d) from WSW during a storm.

Therefore, the objective of this short contribution has been to assess the flood risk of an island beach (Komi, Chios; Fig. 1), using readily available geo-spatial information and an open - source numerical model. Komi is a 1.2 km long barrier beach with a maximum dry width of 38 m. Its backshore hosts a coastal road and many residential and touristic assets, sometimes at a distance of <10 m from the coastline. The beach is characterized by low slopes with elevations that in many areas do not exceed 1.5 m (slopes of approximately 3%). In addition, the backshore elevations are in many areas <1 m. A stream is present at the western segment of the beach, whereas at its eastern end there is a small fishing port. The stream is the outlet of the Katraris river, the land sediment supply of which has been diminished due to the construction of the Kalamoti-Katraris Dam (Andreadis *et al.*, 2021).

Methods

In addition to the simple static inundation 'bathtub' model, a simplified two-dimensional finite difference hydrodynamic model LISFLOOD-FP (Bates and de Roo, 2000) was also used. This simulates flood dynamics in a pre-designed grid using a Digital Elevation Model (DEM). Specifically, LISFLOOD-FP applies fluid continuity to calculate the depth at each grid cell while the water flow is channeled along the ground using a simple storage algorithm based on the difference in hydraulic head between adjacent cells (Bates *et al.*, 2005). In each cell, the calculated height of the water surface above the topographic elevation as well as the Manning soil friction coefficient are used to calculate the flow rate. The water flow is described by the momentum conservation and mass continuity equations:

$$h_{(i,j)}^{(t+\Delta t)} = h_{(i,j)}^t + \frac{\Delta t * Q_{(xi,j-1)}^t - Q_{(xi,j-1)}^t - Q_{(yi,j-1)}^t - Q_{(yi,j)}^t}{\Delta x^2} [1]$$

$$Q^t = \frac{q_t \frac{g h_{flow}^t * \Delta t * \Delta (h^t + z)}{\Delta x}}{1 + g h_{flow}^t * \Delta t n^2 * |q^{(t-\Delta t)}| (h_{flow}^t)^{(10/3)} \Delta x} \Delta x [2]$$

where, (Q^t) is the flow at time (t) between cells, calculated using a centered difference scheme resolved in the (x) or (y) direction; (h_{ij}) is the water depth at the center of cell (i, j); (h_{flow}) is the depth between cells where flow is possible; (z) is the topographic height in the cell; (n) is the ground friction coefficient; (g) is the acceleration of gravity; (q) is the flow from the previous time step; and ($\Delta t, \Delta x$) is the width of the cell.

The flood flows are discretized into a grid of square cells, thus allowing the model to represent two-dimensional flows on the ground surface. LISFLOOD-FP results (ascii files) can be easily imported into a GIS environment for further analysis. The model had been originally designed to simulate river floods, but, in recent years, has been also successfully used to simulate coastal floods (e.g., Monioudi *et al.*, 2018; Le Gal *et al.*, 2023).

The DEM of Komi beach used the 'Digital Terrain Model of the LSO25 project' (LSO - Large Scale Orthophotos) of the Hellenic Cadastre, which was constructed using high-resolution aerial photographs (2014-2016). The Cadastre DEM has a resolution of 2 m, which allows capture of both the slopes of the coastal topography and adjacent coastal works with much greater accuracy than the EU-DEM (resolution of 25 m, spacedata.copernicus.eu/documents/20123/121239/GEO1988-CopernicusDEM-RP-001Validation_Report_13.0.pdf). Application of the model at a local level allows the use of this specific spatial resolution with a very reasonable computational cost. The DEM were processed in QGIS software. The Manning friction coefficient was calculated on the basis of the land uses recorded in the Coastal Zone Land Use/Land Cover (LU/LC) geospatial file of the European Copernicus service (<https://land.copernicus.eu/en/products/coastal-zones>). Manual corrections were applied, which mainly concerned the more accurate design of the beach boundaries (and coastal works and port facilities). As an additional check, the corrections were also taken into account in the DEM of the area to ensure that there were no significant discrepancies between the land uses and the topography, e.g. the polygon corresponding to the sea was checked to overlap pixels with zero elevation. Then, a value for the Manning coefficient was entered for each land use, using the calculations of Papaioannou *et al.* (2018).

The model was driven by the projected Extreme Sea Levels (ESLs) for Chios under the RCP8.5 climatic scenario for 2050 and 2100 extracted from the EU-JRC (Joint Research Centre) database <https://webcritech.jrc.ec.europa.eu/SeaLevelsDb> detailed in Vousdoukas *et al.* (2018). ESLs were projected using the numerical hydrodynamic model Delft3D-Flow driven by the wind and atmospheric pressure fields corresponding to the climate conditions

of the RCP4.5 and RCP8.5 scenarios calculated by an ensemble of 8 climate models; model performance was assessed for the period 1980 – 2014 (baseline) driven by wind/atmospheric pressure fields extracted from the ERA – Interim database. The ESLs form the sum of the future long-term relative mean sea level rise (RSLR), the astronomical tide (n_t) and the episodic sea level rise (n_{ce}) due to meteorological tides (storm surge) and the storm wave set-up; the latter, which can be quite significant during an energetic event, is set using a generic approximation of $0.2 H_s$, i.e., of the offshore significant wave height projected for the same scenarios.

Results

The ESLs with return period of 100 years (ESL_{100}) projected for the area were 1.12 m and 1.77 m for 2050 and 2100, respectively. The bathtub model results showed inundation of 70,850 and 128,300 m² for 2050 and 2100, respectively, with maximum flood extent more than 220 m and 260 m.

The projections show that a large part of the area will be flooded (Fig. 2), with maximum flood extents of 118 m and 190 m for 2050 and 2100 respectively. The beach itself is projected to be completely inundated, presenting a flood risk to all assets at its immediate backshore. Already from 2050 the flood appears to significantly penetrate inshore at the western beach, affecting assets along and to the west of the stream. By 2100, the flood is projected to reach >100 m to the east and west of the stream affecting considerable infrastructure/assets, while the small fishing port will be completely flooded. Overall, it is clear that due to the low relief and many backshore infrastructures/assets there is a high flood risk that can cause serious damages/losses, especially if combined floods (i.e., from land and the sea) are considered, which is a likely occurrence during extreme storms.



Figure 2. Flood extent at Komi beach in 2050 (left) and 2100 (right) under the RCP8.5 scenario. The different colors correspond to the estimated beach width that will be flooded.

Discussion and Conclusions

The results show considerable inundation for Komi beach which is projected to be worse by the 'bathtub' approach. However, the static method is considered to overpredict the flood extent, mainly because it ignores bed friction effects on the flood flow as well as its flood inundation predictions for cells are not hydraulically connected with the rest of the flooded area. Similar discrepancies between the two approaches have been found also in other island beaches (Chatzistratis *et al.*, 2024). In general, flood simulations with numerical models appear more appropriate for local scales while on regional assessment the bathtub approach may be used as fine grids for numerical modelling increase substantially the computation cost (Seenath *et al.*, 2016). Moreover, LISFLOOD-FP provides outputs of flood characteristics at user defined timesteps, providing significant information for flood risk preparedness.

It should be noted that the coastal flood risk in Komi is likely to be exacerbated by the beach erosion/retreat due to the relative sea level rise (RSLR). Andreadis *et al.* (2021) have estimated that Komi beach retreat due to the RSLR will be 3-9 m and 6-9 m by 2050 and 2100, respectively, even under the moderate RCP4.5 climatic scenario. It is noted that these beach erosion/retreat projections are even more conservative, as they

do not take into account the (cumulative) effects of storm events (which, both observations and modeling suggest, could be significant at Komi beach), or the effects of the diminished land-sourced sediment supply due to the construction of the Kalamoti-Katraris Dam. Therefore, in order to assess the flood risk more accurately, coupled beach erosion/flood models will be required. Although such models present large challenges, particularly due to uncertainties at the land/sea boundary condition, future efforts should be focused on it as a response to the major flood disaster risks under climate change.

Acknowledgements

This work was supported by the Project 'Coastal Environment Observatory and Risk Management in island Regions AEGIS+' (MIS 5047038), implemented within the Operational Programme 'Competitiveness, Entrepreneurship and Innovation' (NSRF 2014-2020), co-financed by the Hellenic Government (Ministry of Development and Investments) and the European Union (European Regional Development Fund).

References

- Almar, R., Ranasinghe, R., Bergsma, E.W.J. *et al.*, 2021. A global analysis of extreme coastal water levels with implications for potential coastal overtopping. *Nat. Commun.* 12, 3775. <https://doi.org/10.1038/s41467-021-24008-9>
- Andreadis, O., Chatzipavlis, A., Hasiotis, T., Monioudi, I., *et al.*, 2021. Assessment of and Adaptation to Beach Erosion in Islands: An Integrated Approach. *J. Mar. Sci. Eng.* 9(8), 859. <https://doi.org/10.3390/jmse9080859>
- Bates, Paul D., De Roo, A.P.J., 2000. A simple raster-based model for flood inundation simulation. *J. Hydrology* 236, 54-77 [https://doi.org/10.1016/S0022-1694\(00\)00278-X](https://doi.org/10.1016/S0022-1694(00)00278-X)
- Bates, P., Dawson, R., Hall, J., *et al.*, 2005. Simplified two-dimensional numerical modelling of coastal flooding and example applications. *Coast. Eng.* 52 (9), 793-810. <https://doi.org/10.1016/j.coastaleng.2005.06.001>
- Brett, R., 2021. How Important Is Coastal Tourism for Island Nations? An Assessment of African and Indian Ocean Islands. *J. Coast. Res.* 37, 568–575. <https://doi.org/10.2112/JCOASTRES-D-20-00011.1>
- Chatzistratis, D., Monioudi, I., Velegrakis, A.F., Chalazas, Th., Tragou, E., 2024. Exposure to coastal erosion and flooding in the Northeastern Aegean islands, Greece, in Briand F. (Ed.), *CIESM Monograph 52, Marine hazards, coastal vulnerability, risk (mis)perceptions – a Mediterranean perspective*, CIESM Publisher, Paris, Monaco, 115- 130.
- IPCC, 2023. *Climate Change 2023: Synthesis Report. Contribution of Working Groups I, II and III to the Sixth Assessment Report of the Intergovernmental Panel on Climate Change*, Core Writing Team, Lee, H., Romero, J. (Eds.), IPCC: Geneva, Switzerland.
- Le Gal, M., Fernández-Montblanc, T., Duo, E., Montes Perez, J., Cabrita, P., Souto Cecon, P., Gastal, V., Ciavola, P., Armaroli, C., 2023. A new European coastal flood database for low–medium intensity events. *Natural Hazards and Earth System Sciences* 23, 3585–3602. <https://doi.org/10.5194/nhess-23-3585-2023>
- Luijendijk, A., Hagenaars, G., Ranasinghe, R. *et al.*, 2018. The State of the World's Beaches. *Sci. Rep.* 8, 6641. <https://doi.org/10.1038/s41598-018-24630-6>
- Monioudi, I.N., Asariotis, R., Becker, A., *et al.*, 2018. Climate change impacts on critical international transportation assets of Caribbean Small Island Developing States (SIDS): the case of Jamaica and Saint Lucia. *Regional Environmental Change* 18, 2211-2225. <https://doi.org/10.1007/s10113-018-1360-4>
- Papaioannou, G., Efstratiadis A., Vasiliades, L., Loukas, A., Papalexiou, S.M., Koukouvinos, A., Tsoukalas, I., Kossieris, P., 2018. An operational method for flood directive implementation in ungauged urban areas. *Hydrology* 5, 24. <https://doi.org/10.3390/hydrology5020024>
- Seenath, A., Wilson, M., Miller, K., 2016. Hydrodynamic versus GIS modelling for coastal flood vulnerability assessment: Which is better for guiding coastal management? *Ocean & Coastal Management* 120, 99-109. <https://doi.org/10.1016/j.ocecoaman.2015.11.019>
- Toimil, A., Losada, I.J., Álvarez-Cuesta, M., Le Cozannet, G., 2023. Demonstrating the Value of Beaches for Adaptation to Future Coastal Flood Risk. *Nat. Commun.* 14, 3474. <https://doi.org/10.1038/s41467-023-39168-z>
- UNWTO, 2024. *International Tourism Highlights*. World Tourism Organization: Madrid, Spain, ISBN 978-92-844-2579-2.
- Vousdoukas, M.I., Mentaschi, L., Voukouvalas, E., *et al.*, 2018. Global probabilistic projections of extreme sea levels show intensification of coastal flood hazard. *Nat Commun* 9, 2360. <https://doi.org/10.1038/s41467-018-04692-w>